Ocean Engineering 172 (2019) 46–58

Contents lists available at ScienceDirect

Ocean Engineering

journal homepage: www.elsevier.com/locate/oceaneng

Method for Real-Time Hybrid Model Testing of ocean structures: Case study on horizontal mooring systems

S.A. Vilsen[a,b,*], T. Sauder[a,b], A.J. Sørensen[a], M. Føre[b,c]

[a] Centre for Autonomous Marine Operations and Systems (NTNU AMOS), Department of Marine Technology, NTNU, NO-7491, Trondheim, Norway
[b] SINTEF Ocean, P.O. Box 4762 Torgard, NO-7465, Trondheim, Norway
[c] Centre for Autonomous Marine Operations and Systems (NTNU AMOS), Department of Engineering Cybernetics, NTNU, NO-7491, Trondheim, Norway

ARTICLE INFO

Keywords:
Real-time hybrid model testing
Marine hydrodynamics
Ocean structures
Cyber-physical systems

ABSTRACT

This paper presents a method for Real-Time Hybrid Model testing (ReaTHM testing) of ocean structures. ReaTHM testing is an extension to traditional hydrodynamic model-scale testing, where the system under study is partitioned into physical and numerical substructures. The physical and numerical subsystems are connected in real-time through a control system. Based on experience with various ReaTHM tests, a general method for ReaTHM testing of ocean structures has been proposed. An experimental case study was carried out to illustrate the proposed method. The study was conducted in a state-of-the-art hydrodynamic laboratory, where a physical cylindrical buoy was placed in a still-water basin. Horizontal mooring loads from a numerical mooring system, which were modelled using the nonlinear finite element software RIFLEX were actuated onto the physical substructure. System performance was verified through comparison with a physical horizontal mooring system consisting of physical springs.

1. Introduction

Ocean structures are dynamic systems governed by different physical regimes, where applications can range from e.g. offshore wind turbines, deep sea oil and gas, and aquaculture. Numerical simulations will often be insufficient to fully describe the complex hydrodynamics encountered in the design of ocean structures due to phenomena such as slamming, wave-current interactions and viscous effects. Most ocean structures are therefore experimentally tested for design verification, model validation and load determination. However, conventional experimental test methods will encounter challenges when studying multi-physical systems with phenomena founded in different physical laws. The scaling of phenomena dominated by gravitational effects (Froude scaling) is incompatible with scaling of friction dominated effects (Reynolds scaling) (Newman, 1977). This was exemplified in model scale testing of floating offshore wind turbines, where scaling of the wave field and wind forces are incompatible (Bachynski et al., 2016). Ill-conditioning can arise e.g. in model scaling of the geometry of very long and slender structural members, or in interaction between systems with slow and fast dynamics. Furthermore, when studying structures on very deep water, the general spatial constraints of basins may limit the capabilities of conventional test methods. This has lead to the proposal of using real-time hybrid test methods in the design validation of ocean structures. The denomination Real-Time Hybrid Model testing (*ReaTHM® testing*) is used to specify the use of hybrid testing within the hydrodynamic model scale testing field.

In ReaTHM testing, the emulated system (i.e. the system sought replicated in the model test) is separated into numerical and physical substructures that are interconnected in real-time through a control system (Fig. 1). Real-time hybrid testing was originally developed as an extension to the pseudo-dynamic testing of systems and components in earthquake design analysis of civil engineering structures (Nakashima et al., 1992). The method was developed in order to analyse highly nonlinear and rate-dependent components connected to linear structural Finite Element (FE) analyses. This has been studied extensively within the seismic civil engineering community. Fundamental questions such as stability, interface connection and numerical substructuring have been addressed by (Carrion and Spencer, 2007; Terkovics et al., 2016), while the effect and compensation for time delays were presented by (Horiuchi et al., 1996, 1999; Chae et al., 2013). Similar parallel developments have been made in the Aerospace and Automotive engineering communities through Hardware-in-the-Loop (HiL) testing of control systems on physical hardware and Model-in-the-Loop (MiL) testing of structural members (Plummer, 2006).

* Corresponding author. Centre for Autonomous Marine Operations and Systems (NTNU AMOS), Department of Marine Technology, NTNU, NO-7491, Trondheim, Norway.
E-mail address: stefan.vilsen@sintef.no (S.A. Vilsen).

https://doi.org/10.1016/j.oceaneng.2018.10.042
Received 3 January 2018; Received in revised form 4 September 2018; Accepted 23 October 2018

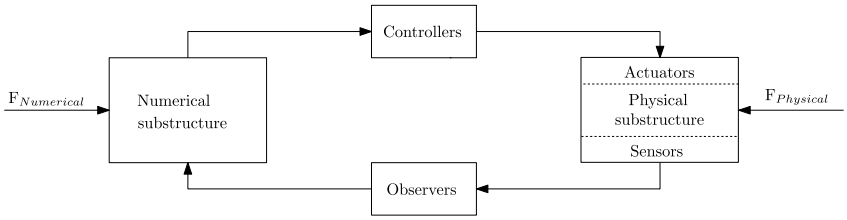

Fig. 1. Schematics of the hybrid testing concept, where the emulated system is separated into one physical and one numerical substructure, with physical and numerical excitation forces. The dynamics of each substructure are transferred using a control system consisting of a sensor-actuator interface.

ReaTHM testing of ocean structures was first suggested as a means for overcoming ocean basin infrastructure limitations when testing ocean structures in deep water applications (Final Report and Recommen, 1998; Buchner et al., 1999; Stansberg et al., 2002). The part of the mooring system that could not be represented physically, and hence had to be truncated (i.e. geometrically divided into substructures), would then be modelled numerically and attached to the physical system through sensors and actuators. These studies were at the time only realised as desktop experiments, as the technology was not yet mature for full implementation due to e.g. insufficient computational power and limited actuator technology.

The research on ReaTHM testing applied to mooring systems has been further developed in more recent studies (Cao and Tahchiev, 2013). ReaTHM testing methods have also been proposed for offshore wind turbines (Chabaud, 2016). One of the main challenges identified for model scale tests of offshore wind turbines is a disparity in scaling regimes as wave-related loads and response should be Froude scaled, while wind-related responses should be scaled using Reynolds scaling. With ReaTHM testing, it is possible to mitigate this challenge by computing the wind loads numerically based on the measured platform motions and simulated wind field and rotor dynamics, which is in itself a challenge (Bayati et al., 2017), and actuate them onto the physical system. Such studies have been conducted both in 5 Degree Of Freedom (DOF) (Sauder et al., 2016; Chabaud, 2016) and 1 DOF (Oguz et al., 2018). A stepwise method for designing a ReaTHM test for offshore floating wind turbines was presented by Sauder et al. (2016).

The research objective of the work presented in this paper was to develop a more formal method for Real-Time Hybrid Model testing of ocean structures. The main scientific contribution of this study is the development of the formal method for performing ReaTHM testing of ocean structures. This study includes a reformulation of the design steps from Sauder et al. (2016) such that they are more general, and hence applicable to a wider range of ocean structures. The method was implemented and tested in a case study of a moored floating structure in the Marine Cybernetics Laboratory (MC Lab) at the Norwegian University of Science and Technology (NTNU), representing a typical application with slender structures (e.g. mooring lines and risers). The control system components used in the case study were developed in a previous study (Vilsen et al., 2017a). Due to the spatial limitations of the basin, a proper physical validation test of a real mooring system would be infeasible. The case study was therefore based on a simplified emulated system that was possible to set up both as a real-time hybrid test and as a purely physical system.he paper is organized as follows: Section 2 presents the general strategy and method for a ReaTHM test. A case study on horizontal mooring systems is presented in Section 3 along with a physical verification study. Finally the results are presented in Section 4 and discussed in Section 5, before concluding in Section 6.

2. Method

Since the primary motivation for the development of ReaTHM testing is to enable testing of ocean structures that are difficult to study in purely physical laboratory experiments, the initial considerations and studies to be performed are similar to those typically done for traditional hydrodynamic model scale testing, i.e. identifying the dynamic system, physical phenomena, scaling regimes and quantities of interest. With this as a basis, and by generalising the design steps for offshore wind turbines presented by Sauder et al. (2016), it is possible to derive a design and execution method for ReaTHM testing of ocean structures. The following design steps are proposed:

1. Identify the dynamic system and governing physical laws
2. Identify the quantities, and temporal/spatial domains of interest
3. Identify ill-conditioning and other constraints in model testing
4. Choose a substructuring- and control strategy
5. Perform a fidelity analysis given physical constraints and substructuring
6. Design and tune the control system
7. Perform verification tests

In the following, the seven design steps are described in detail. A chart of the design procedure is presented in Fig. 2, where the steps are categorized into an initial planning phase, an analysis phase by numerical simulations, and a design and test phase where physical hardware is included.

2.1. Identification of the dynamic system and governing physical laws

It is essential to identify the physical laws governing the system, or the phenomena acting upon it, as these will determine how the system properties should be scaled in physical model representation. In marine technology, a wide span of different applications are possible. Relevant systems may include offshore wind turbines, liquid sloshing in tanks, moored offshore oil & gas and aquaculture structures, tension leg platforms and other slender structures such as pipelines and risers. General characteristics of each structure and system may vary for the different applications and sites of operation. The physical quantities of importance will also depend on which governing physical laws are dominating the system dynamics. Examples of such laws include the symmetry laws of conservation and continuity, laws of motion such as gravitational laws or general Newtonian mechanics, and thermodynamic laws.

2.2. Identification of quantities, and temporal/spatial domains, of interest

The Quantities of Interest (QoI) and the temporal/spatial Domains of Interest (DoI) for a system must be identified to determine where and how to monitor the system in model scale representation. The QoIs are physical quantities of the system which are desired to be directly or indirectly observed in model testing. Examples of relevant QoIs for ocean structures are motions and mooring forces. The spatial DoI is the spatial extent and location of the QoIs. Identifying the spatial domain is important for the truncation between the numerical and physical system and thereby placement of sensors and actuators. Examples of the spatial DoIs are the above water surface structure (wind turbines), the water column (deep water applications), the wave zone and the free surface area. Temporal DoIs are the frequency span and resolution of the QoIs and physical phenomena acting on the system, and are necessary for designing the numerical model, control and actuation system, and logging system. Examples of the temporal DoIs are wave frequencies (1st order), low frequency (2nd order), high frequency such

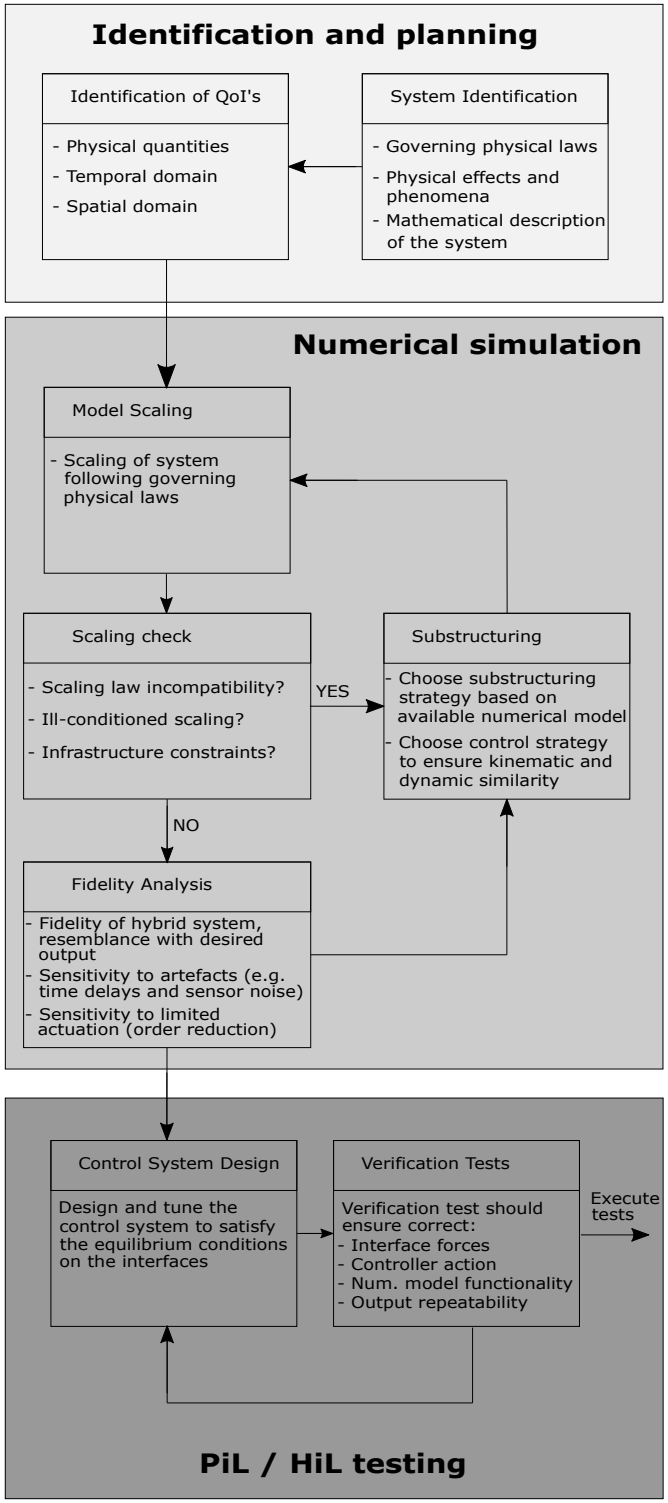

Fig. 2. Flowchart of the proposed design method for ReaTHM testing.

as Vortex Induced Vibrations (VIV) and rare events (such as slamming).

QoIs and temporal and spatial domains are possible to derive based on the identified dynamic system and physical laws important for the system (Section 2.1).

2.3. Identification of ill-conditioning and constraints

In model scale representation of the system, incompatibilities or ill-conditioning of certain properties in the system may render traditional scaled model testing infeasible, and hence requires that hybrid/component testing methods are applied.

Incompatibilities that arise when scaling the system dynamics according to the identified physical laws should be identified, e.g. when scaling system properties founded in different physical phenomena, thereby requiring use of different scaling laws.

Ill-conditioning in scaled representation of the system can also occur when some part exhibit much faster dynamics than the rest of the system, or when scaling components with very large discrepancies in geometric extent, (e.g. mooring line with length 3000 m and diameter 300 mm). Furthermore, very high scaling ratios may make high quality wave generation difficult. The experimental model scale representation of the system can also be constrained by physical and geometrical constraints set by the available test materials and laboratory infrastructure.

2.4. Substructuring- and control strategy

The ill-conditioned properties or physical constraints must be compensated for by performing substructuring, that is partitioning the system into numerical and physical substructures, to separate the different physical domains or phenomena. The location of the interface where the substructuring is performed can be chosen based on various factors.

Dynamics too complex to model numerically need to be modelled physically. The validity of available numerical models will also impact how much of the system it is possible to treat numerically. Tuning these numerical models so that they give satisfactory results (e.g. choosing the correct drag coefficients as input before using them in tests) is a crucial and challenging task. Following Froude scaling, time scales with $\sqrt{\lambda}$, where λ is the geometric scale ratio. The time scaling determines the computational requirement for the numerical models, as the numerical substructure must be designed such that it simulates fast while still capturing the system dynamics.

When a substructuring strategy is chosen, the most important and relevant dynamics of the substructures must be transferred across the interface. This requires fulfilment of similarity conditions on the interface(s) to ensure that the dynamics from the substructures are fully coupled (de Klerk et al., 2008). Following e.g. Bond Graph terminology (Karnopp et al., 2006), the exchange of energy between the substructures can be described by the product of the *flow* (e.g. velocity and rotation rates) and *effort* (e.g. force or torque). This is illustrated in Fig. 3, and is obtained by

1) Ensuring compatibility of displacements in one interface direction.
2) Ensuring equilibrium of forces in the other interface direction.

Using this definition, the control system can be designed to use either flow or effort as the control output. The choice might be affected by technical limitations, possible external disturbances, or dynamics of the control system. Time delays and actuator dynamics might affect the controllability (ability to control a state to a desired setpoint) and causality (cause and effect) on the interface, meaning that the control system dynamics could affect the overall dynamics of the coupled system. The actuator and sensor system must be placed such that they do not introduce physical disturbances that influence the fidelity beyond given limits.

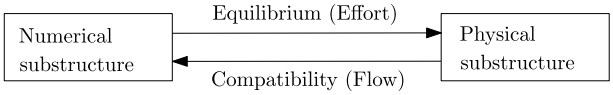

Fig. 3. Similarity conditions on the interface are defined as kinematic compatibility (Flow) in one direction and dynamic equilibrium (Effort) in the other direction. Here the flow is measured, while the effort is actuated.

2.5. Fidelity analysis

The fidelity of a ReaTHM system describes how well the hybrid system represents the emulated system. A thorough definition of the fidelity will be given in (Sauder et al., Sørensen) while (Sauder et al., 2018) contains a more relevant version for marine applications. Sufficiently high fidelity in a test method is necessary for the design validation of ocean structures in order to ensure validity of the test results. For ReaTHM testing artefacts in the system such as actuation errors or measurement noise, may affect the overall behaviour of the system. For high fidelity to be ensured, the quantities of interest should not be affected by such effects. A sensitivity analysis must therefore be performed to identify which artefacts or error sources play the largest role in determining the fidelity of the system (Sauder et al., 2018).

Investigation of the sensitivity to artefacts is possible by developing numerical proxies of the physical subsystem and the interface, and using these to set up a numerical-numerical system emulating the full hybrid test setup (Bachynski et al., 2015; Sauder et al., 2017). The outcome of the fidelity analysis should specify the system requirements for e.g. sensor noise/bias, time delays and numerical model efficiency to achieve the desired fidelity level.

2.6. Control system design

In general, the term “control system” encompasses everything connecting the physical and numerical substructures, including sensors and actuators. The control system should be designed so that it fulfils the requirements derived in Sections 2.4 and 2.5. The physical system must be equipped with a sensor system, such that it is possible to measure or estimate the states or outputs of the physical substructure needed as inputs to the numerical model and in some cases for the control system as well. The sensor system should further give access to the states necessary for observing, evaluating or estimating the QoIs of the physical system. The sampling frequencies should be chosen based on the identified temporal resolution and relevant sampling theorems. Similarly, the control system should run fast enough to avoid any shortcomings in the model and signal reconstructions, and aliasing. The sensor system can for instance include both analogue and digital sensors with different sampling/update frequencies. Continuous time signals should then be properly reproduced for input to the numerical substructure by using interpolation and extrapolation methods, e.g. Zero-Order Hold.

As mentioned earlier, the control system performance can be affected by artefacts such as time delays, scaling errors, sensor bias and noise, wild-points and drift. Time delays are particularly critical to system performance as they may induce errors or instability 7. To fulfil the equilibrium condition the corresponding force from the numerical model must in principle be applied at the same instant the measurement is made. This is not practically possible, due to e.g. non-zero time delays from communication, numerical computation, and actuator dynamics. The aim is therefore to:

1) Minimize time delays when possible.
2) Identify and compensate for time delays in the system.

An actuation system should ensure that the desired loads, or displacements (depending on the selected actuation strategy) from the numerical substructure is actuated onto the physical substructure. Actuated quantities must be measured or estimated for traceability and feedback to the controllers. This feedback must be fast enough to follow the reference without inducing artefacts in the form of time delays or actuation errors. Note that other types of artefacts than time delays cab be of importance, e.g. force sensor calibration errors (Sauder et al., 2018).

2.7. Verification tests

The performance of a ReaTHM test setup must be verified before it can be used as a basis for the design validation of ocean structures. However, verification is often a non-trivial task, as artefacts may induce variations in the dynamics of the coupled physical/numerical system that are difficult to directly observe and quantify. Verification studies should therefore systematically test the system functionality to quantify if any errors are induced through artefacts or system dynamics. Such test schedules may include:

- The *interface connection* between the numerical and physical substructures must be examined to verify e.g. that interface quantities and coordinate transformations are correctly transferred.
- *Controller actions* should be verified through static and dynamic tests.
- The *numerical model* used in real-time (with sensor input) must be verified by studying quantities such as jitter/time lags, clock synchronization and output noise.
- *Repeatability* of the output and QoIs should be verified by performing several tests in the same conditions.
- *Time delays* in the system should be quantified to verify the compensation scheme and ensure traceability of the induced delays/errors.
- All *monitored artefacts* should be within bounds defined in Section 2.5.

Further verifications may include test of robust error handling and safety measures to avoid sending undesired commands to the actuators that may damage technical equipment.

Validation tests of a ReaTHM testing setup, where the performance of a purely physical laboratory experiment equivalent to the hybrid setup is compared with the ReaTHM test output should also be performed before the system is used for actual studies. The core functionalities of the system, and key parameters such as time delays, allocation and controller action should then be validated against a reference system that is possible to set up as a purely physical system.

3. Case study: horizontal mooring systems

The stepwise method presented above was formulated as a general approach in order to design hybrid test setups for ocean structures. However, the specific design steps from idea to experiment will vary from system to system. In the following, the ReaTHM testing method is applied to a case study focused on horizontal mooring of a cylinder buoy. No external environmental loading (waves, current, wind) were acting on the system in this study, only static displacement tests and free decay tests were performed. However, the system was developed to satisfy requirements for future studies with wave excitations.

3.1. Identification of the dynamic system and governing physical laws

The *emulated* system was a moored floating cylinder buoy, with a mooring system consisting of 12 mooring lines attached to its circumference. This buoy has previously been used in studies where the keel geometry was varied (Vilsen et al., 2017a). A rounded corner geometry was used in the present study. This system was chosen as a case study because the test campaign should serve as a principal study of the method, while at the same time maturing the technology by introducing challenges that have not previously been addressed with respect to ReaTHM testing.

The choice of a generic cylindrical shape gives a flexibility in testing, as the hydrodynamic properties are then isotropic. This also means that the methods developed will not be very application specific, but can be utilized for testing any rigid floating structures, e.g. offshore oil and gas or aquaculture systems.

Table 1
Main parameters of the cylinder buoy in model and full scale given as geometric extend, mass, estimated hydrodynamic added mass and linearised equivalent damping. Main parameters of the mooring system given as the depth is the water depth at the location, the radius of the mooring system excluding the radius of the floater, the length of one cable, the number of lines and the total horizontal stiffness of the full mooring system at the origin.

Cylinder Buoy	Full scale	Model scale
Radius [m]	43.2	0.30
Draft [m]	14.4	0.10
Volume [m^3]	$7.44 \cdot 10^4$	$2.49 \cdot 10^{-2}$
Mass [kg]	$8.62 \cdot 10^7$	28.2
Added mass [kg]	$3.81 \cdot 10^7$	12.5
Damping [kg/s]	$6.18 \cdot 10^6$	24.2
Mooring System		
Depth [m]	320	2.22
Radius [m]	1494.5	10.4
Line length [m]	1567	10.9
Nr lines	12	12
Total stiffness [N/m]	$282.6 \cdot 10^3$	13.3

For the case study to function as a benchmark test for hybrid model testing, the scaling ratio was set very high at $\lambda = 144$. This resulted in a time scale ratio of 1:12, which set a high requirement for the simulation speed of the high fidelity and possibly complex numerical substructure. Using a high scaling ratio also increased scaling- and measurement uncertainty for the tests. However, as the primary research objective of the case study was to implement and study the performance of the ReaTHM test setup, the added experimental uncertainty was not of primary concern. The properties of the cylinder buoy and mooring system in full scale and in model scale are presented in Table 1. Parameters of the cylinder buoy determined from inclination tests are presented in Table A4 in the Appendix.

The dominating physical laws and phenomena acting on the system are the inertia and viscous forces on the hull and mooring lines. The equations of motion can be described by the 6 DOF vectorial form presented by (Fossen, 2011), derived from Newton-Euler equations for coupled translational and rotational motions:

$$M(\dot{\nu})\dot{\nu} + D(\nu)\nu + g(\eta) = \tau_{ext} + \tau_{moor} \tag{1}$$

where $\eta \in \mathbb{R}^6$ is the 6 DOF position, given in a local Earth-fixed frame as North-East-Down (NED) coordinates and Euler angles, and $\nu \in \mathbb{R}^6$ is the 6 DOF velocity in the body-fixed frame, given as linear translational velocities and rotation rates. $M \in \mathbb{R}^{6\times6}$ is the mass and added mass matrix of the cylinder buoy, $D \in \mathbb{R}^{6\times6}$ is the damping matrix, $g(\eta) \in \mathbb{R}^6$ is the hydrostatic stiffness vector, and $\tau_{ext} \in \mathbb{R}^6$ and $\tau_{moor} \in \mathbb{R}^6$ are the external and mooring force vectors and moments acting on the buoy, respectively.

For this type of system, model testing is needed to identify the viscous drag and eddy making near the surface of the body, which are challenging to compute numerically. In decay testing, the system may in rough terms be considered by only studying 1 DOF motions of the floater in the decay direction (isotropic parameters). The matrices (1) then reduce to one equation, with mass, stiffness and damping as given in Table 1. The linearised viscous damping estimate is averaged over one oscillation period for an excursion of 1.5 cylinder radius.

3.2. Identification of quantities, and temporal- and spatial domains, of interest

The QoIs are the oscillation period of the floating cylinder, the top tensions in the mooring lines and the damping of the coupled system (linear and quadratic damping coefficients p_1 and p_2). These quantities are related to the static and dynamic properties of the mooring system

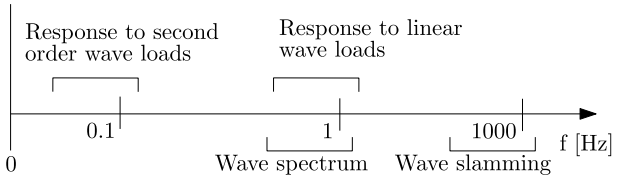

Fig. 4. Frequencies of interest of the system in model-scale quantities.

Table 2
Quantities of interest of the system in model and full scale.

QoI	Full scale	Model scale
Planned excursion [m]	63	0.45
Restoring force [N]	18.3e6	6.0
Surge/sway period [s]	130	11
Roll/pitch period [s]	12	1

and the hydrodynamic added mass and damping. As the system operates in full scale for the numerical substructure and model scale for the experimental substructure, temporal and spatial resolutions change across the interface. The maximum excursion applied was 1.5 times the radius of the cylinder, approximately 63 m in full scale and 0.45 m in model scale. The expected oscillation period of the surge motions was near 120 s in full scale and 10 s in model scale, and an expected roll/pitch period 12 s full scale and 1 s in model scale (Fig. 4). The tangent stiffness of the mooring system at the origin was 282.6 kN/m in full scale. With the expected excursion this gives a maximum mooring force of approximately 18.3 MN in full scale and 6N in model scale (Table 2). For future applications that include wave forces, a wave spectrum with significant wave height of 14 m and peak period of 12s in full scale would result in 0.1 m and 1s model scale parameters.

3.3. Identification of ill-conditioning and constraints

The ill-conditioning of the dynamic system mainly consists of the radically different dimensions between the mooring system and the topside floating structure. The large spatial extent of the mooring system, 1494.5m radius for a single mooring line and 320m water depth, requires a scaling ratio of 1:250, to fit the constraints of the 6m wide basin infrastructure. Such a large scaling ratio is not feasible for observing the hydrodynamic effects on the floater (Stansberg et al., 2002). Another aspect is that soil-structure interaction occurs as mooring lines are lifted and lowered on the seabed, which might be difficult to reproduce in physical model testing.

3.4. Substructuring- and control strategy

The substructuring was desired was set up to compensate for the geometric constraints in the laboratory infrastructure while retaining the complex flow regimes at the free surface. The numerical nonlinear FE software RIFLEX (Ocean, 2016) was chosen to simulate the parts of the mooring system that did not fit in the basin. The software has been thoroughly documented and validated, and is thus considered sufficiently accurate to represent such mooring systems (Aksnes et al., 2015). For simplicity, the coupling on the interface was reduced to the 2 DOF horizontal force components. The vertical force component was excluded, as the effect on decay testing in still water can be neglected. However, it may be of importance for other applications such as semi-submersibles, especially when damaged stability is in focus. As only the horizontal force components were transferred, and no physical part of the mooring lines were present in the tests, the truncation point can be considered as the fairled points of the cylinder, such that the entire mooring system was modelled numerically. Using the definition of truncation ratio given by (Sauder et al., 2017) (i.e. truncated length

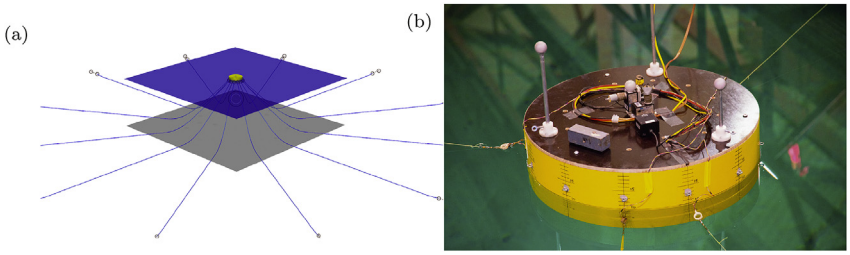

Fig. 5. (a) Visualization of the numerical substructure, as modelled in RIFLEX. (b) The physical substructure with attached load cells on the actuation lines, reflective markers for optic position measurement and on-board acceleration measurement.

divided by total length), this resulted in a truncation ratio of 1. The mooring lines were designed with four segments, a top chain segment, a fibre rope segment, a heavy chain segment near the mud-line and a long chain segment to the anchor, each line being modelled by 60 elements distributed over the four segments. The full model contained 720 elements. The input values for the numerical model are presented in the Appendix (Table A.5), with the longitudinal and lateral drag coefficients used in the Morison equation for determining the hydrodynamic loads.

To satisfy the similarity conditions stated in Section 2.4, a control strategy should be designed to control either the position/velocity (flow) of the cylinder buoy or the force (effort) exerted upon the buoy. As the response of the physical system to the hydrodynamic forces is a QoI, the physical model should be able to interact freely with the hydrodynamic forces (i.e. the dynamics remain undisturbed). Inertia dominated hydrodynamic forces on the cylinder depend on the acceleration, i.e. the relative difference between the acceleration of the fluid and the cylinder.

If the position and velocity were to be controlled, the measured acceleration would need to be correct as well to achieve correct forces. This is challenging due to effects such as measurement errors, actuator dynamics and time delays.

In contrast, if force control is applied, the cylinder can be controlled to better interact with the environmental forces by adding a compliant element and actively compensate for external disturbances (disturbance rejection). The restoring forces from the numerical substructure are then actuated onto the system separately. Induced errors or delays will then primarily be in the form of errors in the mooring force, and not directly impact the hydrodynamic forces.

Based on these observations, force control was chosen for the case study, with the measured position and velocities being input to the numerical substructure, and calculated forces being actuated onto the experimental substructure. The actuated DOF's were then reduced to the horizontal NE-components of the force computed by the numerical substructure.

3.5. Fidelity analysis

One artefact in the case study is the reduced order of coupling on the numerical-physical interface. The substructure interface should ideally be designed to transfer the 6 DOF dynamics between the substructures. However, the actuation of interface forces was limited to the 2 DOF horizontal force resultants, for simplicity. In the case study, only horizontal translational motions are considered, where the stiffness from the mooring system can be described by the catenary effect. Further, the total mass of the mooring system is small compared to the mass of the floating cylinder. This means that the horizontal force resultants play the largest contribution, while the influence of the vertical forces can be neglected (Faltinsen, 1990).

The physical substructure (buoy) had no stiffness in the horizontal plane besides that supplied by the numerical mooring system. This meant that even small errors in the position and force measurement system would affect the overall dynamics. Further, the system had a high scaling ratio, and was sensitive towards scaling errors or dimensional errors, as 1 N error in force measurement/actuation in model scale results in ca 3 MN error in full scale.

Due to the rounded corner geometry of the cylinder buoy, very little physical damping was present in the ReaTHM setup. The system was therefore sensitive to time delays in the control system (Horiuchi et al., 1999; Ueland and Skjetne, 2017).

3.6. Control system design

The architecture of the real-time system was developed to accommodate the equilibrium and compatibility requirements on the interface (see Section 3.4). Details on the control system algorithm have been presented in Vilsen et al. (2017a), while the individual system functionalities are presented here (Fig. 6).

3.6.1. Sensor system

The physical substructure was placed at the center of the test basin, and equipped with a sensor system consisting of an optical position measurement system, three-component accelerometers and load-cells on the actuation lines (Fig. 5b). The optical positioning system logged

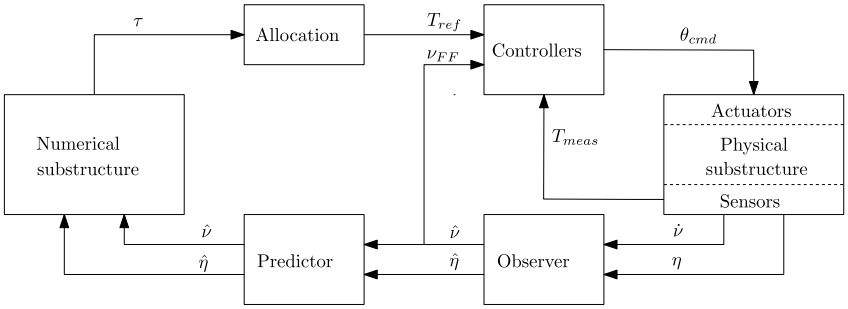

Fig. 6. The architecture of the control system is presented: A sensor system outputs the 6 DOF position (η) and the 3 DOF accelerations (a). An observer estimates the 6 DOF position ($\hat{\eta}$) and 3 DOF velocity ($\hat{\nu}$), a predictor compensates for time delay, numerical model, allocation procedure, controllers and actuation system.

the rigid body position and attitude of the physical substructure at a update rate of 100 Hz given in NED coordinates with respect to a local earth-fixed (inertial) reference system. The accelerometers were placed on deck to measure the surge-, sway- and heave accelerations of the physical substructure with respect to a body-fixed (non-inertial) reference system at a sampling rate of 300 Hz. A data acquisition system was placed inside the buoy for logging the sensor data. The sensor data was timestamped to ensure traceability of time delays, and sent to a control system on land through optic fiber wire.

3.6.2. Kinematic observer

The measured states of the physical substructure were 6 DOF position and attitude, and 3 DOF linear accelerations. Translational velocities are needed as input for the numerical models and for the controllers, and are ideally obtained by integrating the accelerations. However, sensor bias in the accelerometers may then induce drift in the integrated values which may in lead to divergence. Hence, a kinematic observer was implemented to estimate the states of the system through fusion of different sensor inputs. A nonlinear passive observer for Inertial Measurement Unit (IMU) and Global Navigation Satellite System (GNSS) integration was chosen (Fossen, 2011), using accelerometer- and gyro measurements as proxies for IMU-data, and optical position measurements as proxies for GNSS-data. The observer outputs were the estimated position and instantaneous velocity, along with the sensor bias for the accelerometer. Implementation of the observer has previously been described in 18, and the details can be found in Appendix A.3.

3.6.3. Prediction

Time delays induced by the measurement system, communication/computation time and actuator dynamics were identified, and a prediction scheme was introduced to compensate for the time delays. Since environmental loads affecting the experimental substructure and hence the motions of the floater are generally not modelled well, it was not possible to use model-based prediction methods. Instead, a polynomial prediction procedure was applied, for predicting future values of the estimated position and velocity.

A third order polynomial approximation was fitted to each individual physical quantity, and prediction performed as polynomial extrapolation. The polynomial identification was performed using the 50 previous data points (250 ms model scale), and extrapolation was done 6 data points ahead, corresponding to a 30 ms prediction in model scale (360 ms is full scale). This prediction window was chosen primarily to compensate for the delay from the position measurement system, without introducing unacceptable overshoot and noise 18.

3.6.4. Controller- and actuation system

The objective of the controller and the actuation system was to apply the loads $\tau \in \mathbb{R}^2$ computed by the numerical substructure onto the experimental substructure. The applied force must satisfy the equilibrium condition on the moving interface, equivalent to the sum of the two main control objectives (Chabaud, 2016):

1) Reference tracking of the desired force
2) Disturbance rejection (actively compensate for external disturbances on the physical substructure)

For the ReaTHM test setup, three actuators were placed in the horizontal plane, with 120° spacing around the physical substructure. The actuation was performed through a system consisting of a rotary actuator (a brushless DC motor) connected to a (compliant) clock spring. The spring excited a pulley wheel which transformed the rotary motion into a translational motion through an actuation wire connected to the experimental substructure. The compliant element was added to reduce the overall stiffness of the actuation system, and thereby reducing the system response to external disturbances.

An allocation procedure was used to calculate the individual line tensions required from each actuator to apply the global load vector τ, which is found by summing the horizontal top tension components from the mooring lines in the numerical substructure. The theory behind this approach is briefly presented in Appendix A.4, and can be found in full length in (Vilsen et al., 2017a).

The first control objective; *Reference tracking of the desired force*, was sought satisfied through two controllers. First, a reference feed-forward controller that used a quasi-static model of the actuation system, to estimate the required actuation command to apply the desired force (T_{ref}). Second, an integral feedback controller that integrates the error between desired and measured force (T_{meas}) to compensate for estimation error and drift in the other controllers. The second control objective; *Disturbance rejection*, was sought satisfied by a velocity feed-forward controller, which used the estimated velocity ($\hat{v}$) of the physical system in the inertial reference frame, to find the elongation velocities of the individual actuation lines (v_{FF}). The elongation velocities were then integrated and the resulting position used to compensate the floater motions through motor commands.

3.7. Verification study

The experiments were conducted at the Marine Cybernetics Laboratory (MCL) at NTNU. The laboratory is a 30 m long and 6 m wide wave basin, with a wave generator at one end, and wave absorption at the other. The depth at the test section is 1.5 m.

When using RIFLEX for simulation of the numerical substructure, nonlinear damping is introduced from hydrodynamic drag on the mooring lines. Furthermore, time delays are introduced from computation time and communication time with the external PC running the simulation. For the verification study, a linear isotropic stiffness model was therefore implemented directly in the control loop instead of using RIFLEX as a numerical substructure. The modelled stiffness was applied without introducing further time delays, and with no damping model included. The performance of the remaining components of the control system could then be tested isolated from the numerical substructure.

3.7.1. Tests performed

Static displacement test were performed to evaluate the allocation procedure and interface connection in the static case, by verifying that the commanded load from the numerical model was correctly applied to the physical system. This was done by applying a stepwise static displacement to the physical substructure and by comparing the applied load to the commanded load.

Dynamic decay tests, during which the buoy was manually pulled away from the equilibrium position and released, were performed to evaluate the dynamic properties of the system, including oscillation frequencies, hydrodynamic damping and applied mooring loads. Several decay tests were performed to verify the repeatability of the results.

3.7.2. Analysis theory

The applied horizontal load was found by using the instantaneously measured line tensions in the three actuation lines. Measured position of the buoy and the known positions of the actuators were first used to obtain the unit vectors of the actuation line tensions. Horizontal North and East components of the applied mooring force could then be found by vector summation.

The expected oscillation periods of the coupled buoy and linear numerical stiffness were estimated by

$$T_0 = 2\pi\sqrt{\frac{M}{k}} \tag{2}$$

where M is the measured total mass of the buoy, plus added mass determined as 0.5 times the displaced volume, and k is the horizontal

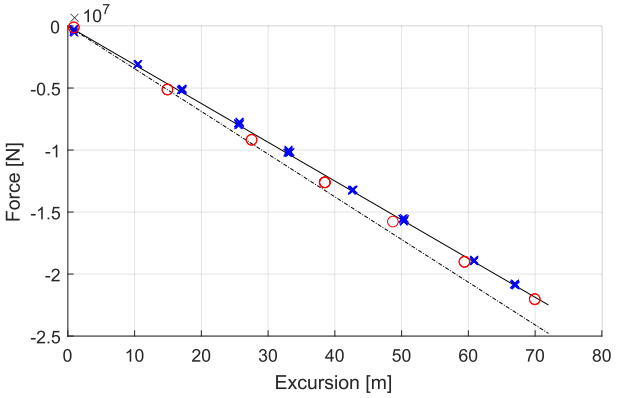

Fig. 7. Mooring-induced restoring force as a function of the excursion of the floater during static displacement test. The restoring force exerted by ReaTHM system (blue crosses), input stiffness to the ReaTHM system (black full-drawn line), measured restoring force exerted by the physical system (red circles) and estimated tangent stiffness at the origin (black dash-dotted line). (For interpretation of the references to colour in this figure legend, the reader is referred to the Web version of this article.)

stiffness of the numerical mooring system.

A method presented by 28 (Cp. 7) was used to estimate the normalized damping coefficients. The equation of motions is normalized, and the linear and quadratic damping is described by coefficients p_1 and p_2, and the stiffness by the coefficient p_3. The 1 DOF equation of motion for a decay can then be stated as:

$$\ddot{x} + p_1\dot{x} + p_2|\dot{x}|\dot{x} + p_3 x = 0 \tag{3}$$

where x is the position/excursion, and $\dot{x}$, $\ddot{x}$ represent first and second derivative with respect to time. Results from decay tests were used to estimate the linear and quadratic damping coefficients by using the relation

$$\frac{2}{T_m} log\left(\frac{X_{n-1}}{X_{n+1}}\right) = p_1 + \frac{16X_n}{3T_m}p_2 \tag{4}$$

where T_m is the oscillation period and X_n is the amplitude of the nth oscillation. The damping coefficients can then be found by performing a decay test and plotting $\frac{16X_n}{3T_m}$ on the x-axis and $\frac{2}{T_m} log\left(\frac{X_{n-1}}{X_{n+1}}\right)$ on the y-axis. The slope of the line gives an estimate of the quadratic damping coefficient, while the crossing with the y-axis gives an estimate of the linear damping coefficient.

The sensor data were sampled in model-scale time at 300 Hz. As the motions of such a system are at much lower frequency bands, the sampled data was low-pass filtered with a cutoff frequency at 4 Hz in model scale, which is equivalent to 0.33 Hz in full-scale. The frequencies that are then filtered out, lie well outside the expected frequencies of both the motion response and the expected external excitations, where little energy would be present at higher frequencies than 0.2 Hz in full scale and 2.4 Hz in model scale (Faltinsen, 1990).

3.8. Validation study

A full physical test using physical horizontal springs to represent the mooring system was performed to validate the ReaTHM test. To validate both the statics and dynamics of the hybrid system, it was desired to design a case that could be tested both experimentally and numerically with high fidelity, and with static and dynamic equivalence between the systems.

The setup was developed such that each actuation line was replaced by a physical spring that was attached horizontally to the buoy, with 120° spacing between individual lines, similarly to the actuation lines for the hybrid system. The initial length of the springs was 2.14 m, and they were subjected to an initial elongation of 0.9 m. The springs were individually pre-tested and rated to have a stiffness of 8.7 N/m. The three-spring system, lead to an initial stiffness of 13.05 N/m, for a pull in a direction in-line with one of the springs (note that the stiffness is anisotropic with this setup). If alternatively considering a vertical spring system using pulleys to apply the horizontal stiffness, friction damping would be induced by the pulleys. This is a problem, as the damping of the system is a QoI.

3.9. Tests using RIFLEX

After verification and validation tests, a test series was performed with the fully nonlinear FE model as numerical substructure. As in the verification test, both static and dynamic tests were performed.

4. Experimental results

This section presents the results obtained through experimental testing.

4.1. Static displacement tests

Results from the static displacement tests are presented as the measured applied restoring force resulting from a stepwise excursion (Fig. 7). The measured stiffness from the verification study corresponds well with the desired stiffness given as input for the linear stiffness model.

The static results from the validation study show a higher initial stiffness, gradually sloping towards the same stiffness as that applied in the verification study.

4.2. Decay and repeatability

Results from three repetitions of decay tests are presented along with the estimated linear and quadratic damping coefficients for the verification study (Fig. 8) and for the validation study (Fig. 9). The decay results (Figs. 8a and 9a) are presented in terms of the normalized horizontal motions of the floater, along the decay direction. In the damping plots (Figs. 8b and 9b), the full-drawn line indicates a fit to the first 8 oscillation amplitudes of all three tests.

The verification tests demonstrate good repeatability in oscillation period and damping (Fig. 8a), though variations in the oscillation amplitudes resulted in scattering of the estimated p_1 and p_2 between tests (Fig. 8b). Oscillation periods from tests with varying stiffness were systematically lower than the theoretically expected results (Table 3).

The validation test results showed good fit for the quadratic damping coefficient at large amplitudes, while a transition towards linear damping was observed at smaller amplitudes (Fig. 9b).

4.3. Applied load

A time series plot of the applied load during a decay test in the verification study is presented (Fig. 10). The commanded North and East resultants are presented along with the applied load. The applied load in general show good correspondence with the commanded load, though some undershoot is observed. The sampled load signal included high energy content at higher frequencies, which was removed by low-pass filtering of the presented results.

4.4. Tests using RIFLEX

The results of the verification test using the nonlinear FE model RIFLEX are presented for the static and dynamic case (Fig. 11). The results show that the nonlinear geometric stiffness has been applied as intended (Fig. 11a), and that results from dynamic tests are repeatable (Fig. 11b). Top tensions from all twelve simulated mooring lines during a decay test show a variation in individual loading, with highest loads

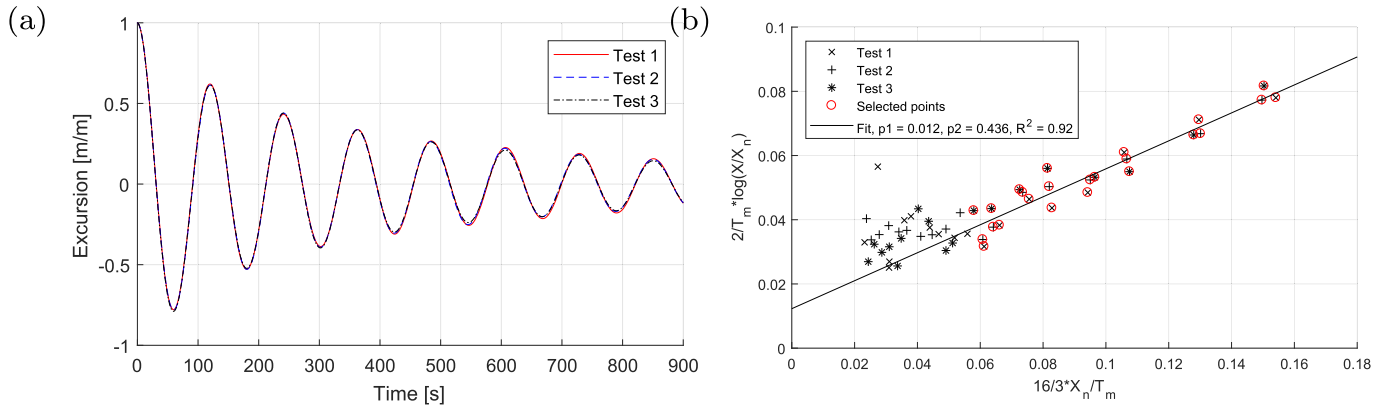

Fig. 8. (a) Three repetitions of decay tests performed with ReaTHM testing and applied linear isotropic stiffness of 14.7 N/m. (b) Linear and quadratic damping coefficients estimated for the decay tests.

for those in-line with the excursion direction (Fig. 12).

5. Discussion

In this section the presented results are discussed and the validity evaluated.

5.1. Verification study

The results of the static displacement tests show that in the static case, the control system was able to apply the correct restoring force. The restoring force was applied by allocating the output from the numerical substructure to the three actuators and applying the allocated setpoints to the controllers. The good correspondence between commanded and applied force implies that the allocation procedure performs well and that the individual line force controllers were able to track the desired static setpoint. If the allocation procedure was not functioning correctly, the static forces would not match for numerical and physical systems.

The good correspondence between the three decay test repetitions imply that the damping and oscillation periods (QoIs) of the system are highly repeatable. Since repeatability in the QoIs is very important for model testing in general, this strengthens the impression that this ReaTHM testing setup performs consistently.

The oscillation periods for the five different stiffness levels tested with the linear isotropic stiffness model in the hybrid system matched well with the theoretical period based on the mass, added mass and stiffness of the system. However, the period applied with the hybrid system is systematically lower than the expected, by approximately 2–5%. This could be because the added mass was lower than theoretically expected, possibly due to the rounded keel geometry.

Table 3
: Full scale measured natural period from ReaTHM testing, compared with the expected period, using mass and added mass for the cylinder.

K [N/m]	T_{meas} [s]	$2\pi\sqrt{\frac{M}{K}}$ [s]	ε [s]	ε [%]
1.53e5	169.0	179.0	−10.0	−5.60
2.70e5	131.2	134.9	−3.7	−2.74
2.83e5	125.8	131.8	−6.0	−4.57
3.12e5	121.8	125.4	−3.6	−2.83
5.83e5	89.3	91.3	−2.0	−2.23

The results of the commanded vs. applied force show that the controller action was able to follow the commanded reference well. There was a systematic undershoot of the applied force, indicating that performance could be improved by applying faster control action. However, the dynamics of the actuation system generates high frequency vibrations which interact with the controllers. By increasing the controller gains, the interaction between vibrations and controller action is amplified. This limits the possible controller configurations with the present system, and indicates that improvements in the mechanical design are needed.

5.2. Validation study

The results from the decay tests in the physical validation study demonstrated good repeatability in oscillation period and damping. The comparison of the horizontal spring system and the results from ReaTHM testing show a difference in the stiffness applied in the tests,

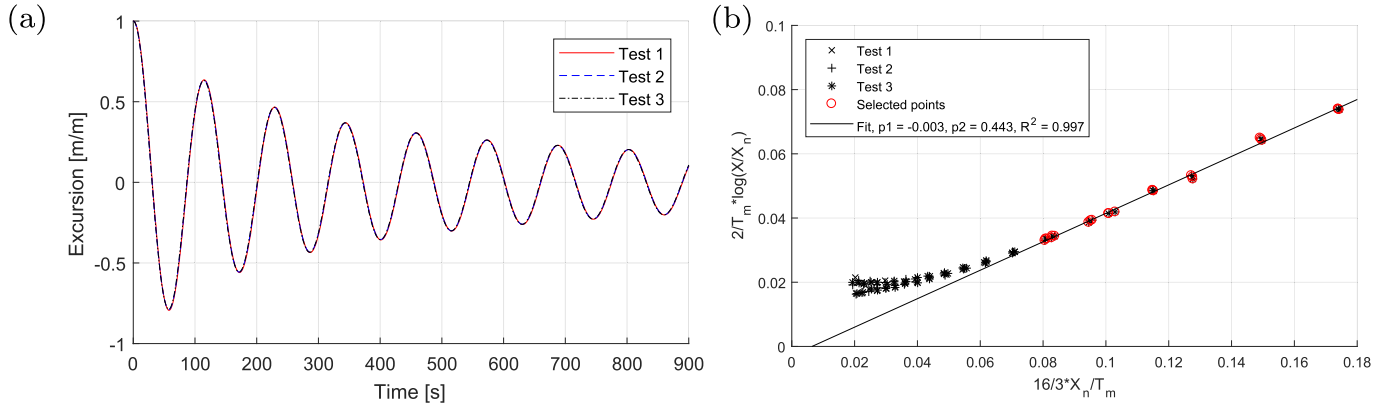

Fig. 9. (a) Comparison of three decay tests with the physical horizontal spring system. (b) Damping coefficients estimated for test with the physical horizontal spring system.

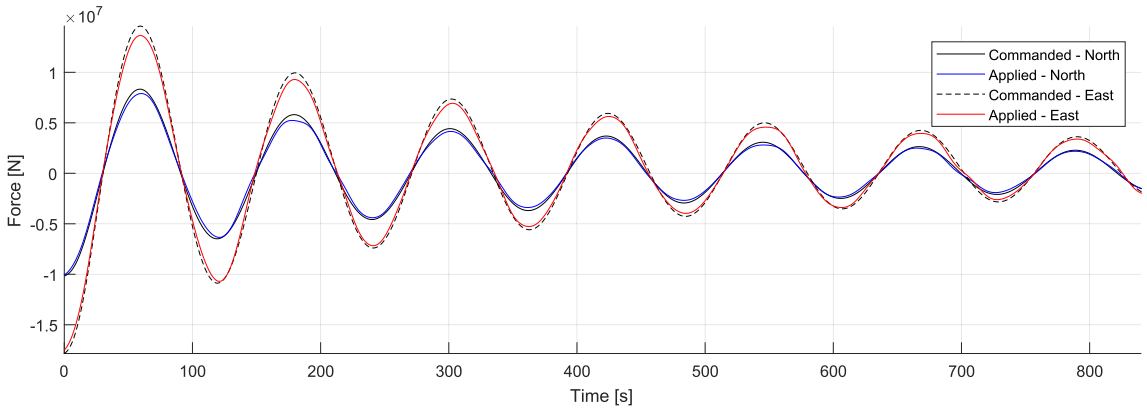

Fig. 10. The commanded force resultants output from the numerical substructure in North-direction (Full-drawn) and East-direction (Dotted) versus the low-pass filtered (cutoff frequency 0.5 Hz) measured actuated force resultants in North component (Blue) and East component (Red). (For interpretation of the references to colour in this figure legend, the reader is referred to the Web version of this article.)

with the physical system exhibiting nonlinear anisotropic stiffness, while the hybrid system was set up with a stiffness based on a theoretical stiffness obtained by using trigonometry and the individual spring stiffnesses. The stiffness of the physical system was measured to be higher than the theoretical value, probably due to the catenary effect of the suspended horizontal springs. Due to the higher physical stiffness observed during testing, the stiffness of the hybrid system was changed to 14.7 N/m, corresponding to the tangent stiffness of the physical system at 1.6 radius excursion. However, this was an underestimation of the stiffness, as the stiffness was higher near the equilibrium point, and the anisotropic properties results in higher stiffness for excursion in the direction opposite to the tested. The difference in stiffness resulted in longer oscillation periods for the hybrid system than for the physical validation tests.

Given the discrepancies between the physical and hybrid system described above, the present case does not serve as a full validation of the system. However, the results can to some extent still be used to validate the system dynamics. As the springs in the physical setup were not in contact with water, and no moving parts were introduced, the springs should ideally not add any damping to the system in both the hybrid and purely physical setups. The damping should therefore purely originate from the hydrodynamic damping of the buoy. However, artefacts in the actuation system, such as time delays or actuator dynamics can appear as additive or dissipative energy in the hybrid system, or negative or positive damping. Comparison of the damping levels of the two systems, can then give an indication of the significance of the artefacts in the hybrid system 29.

The induced damping varies with the velocity, and therefore also by stiffness. By using the method presented in Section 3.7, the damping is normalised with respect to the excursion and the oscillation period. The results presented for the hybrid test and physical test, show that similar linear and quadratic damping levels are present in the two systems. For both studies, the damping is initially purely quadratic, with a close fit to the straight line in the damping coefficient plot. As the velocity decreases, the damping goes towards linear damping. This appears clearer in the physical test, where the shift occurs gradually, beginning from when the maximum velocity during an oscillation drops below 0.1 m/s or equivalent to a Keulegan-Carpenter (KC) number of 1.5. The damping is fully linear from the velocity drops below 0.055 m/s, equivalent to a KC number of 0.95.

Linear hydrodynamic damping arise from viscous skin friction on the cylinder surface, while the quadratic damping is typically associated with eddy-making damping due to flow separation (Faltinsen, 1990). The increased linear damping observed for the hybrid system at very small amplitudes is opposite of what would be expected, since time delays in the system would induce negative linear damping (Ueland and Skjetne, 2017). This could be due to errors in the disturbance rejection, as identified in a previous study (Vilsen et al., 2018). Such effects may modulate the system dynamics due to the control system action.

Further validation and verification studies are needed to prove that the present system will have satisfactory performance in future testing. In addition to investigating the hybrid system's ability to reproduce the system characteristics, stiffness and dynamics, a full validation study should also validate the correct response given a range of relevant

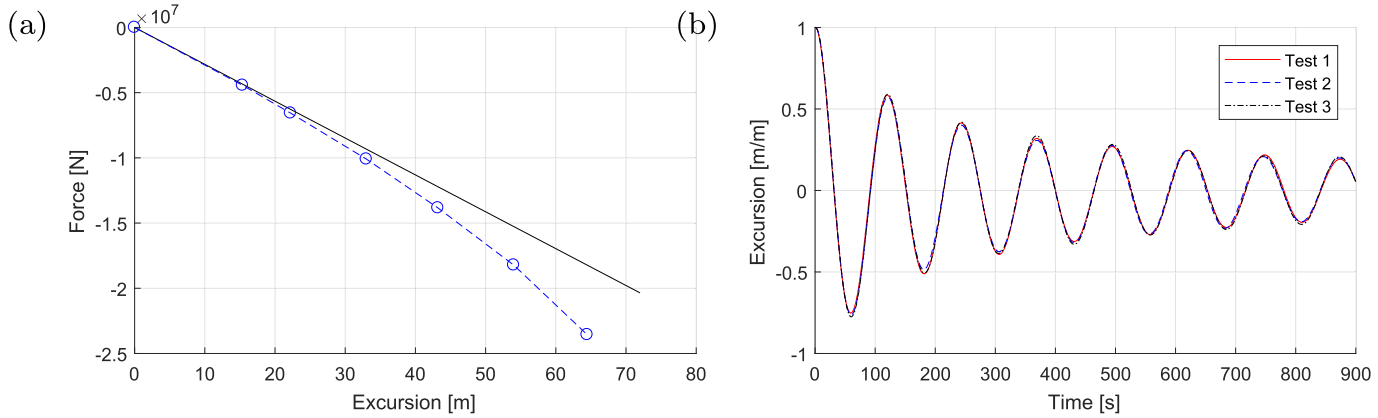

Fig. 11. (a) Static displacement test results with RIFLEX, linear tangent stiffness at the origin (black full-drawn line) and measured applied restoring force (blue crosses). (b) Three repetitions of decay tests performed with ReaTHM testing and RIFLEX as numerical substructure. (For interpretation of the references to colour in this figure legend, the reader is referred to the Web version of this article.)

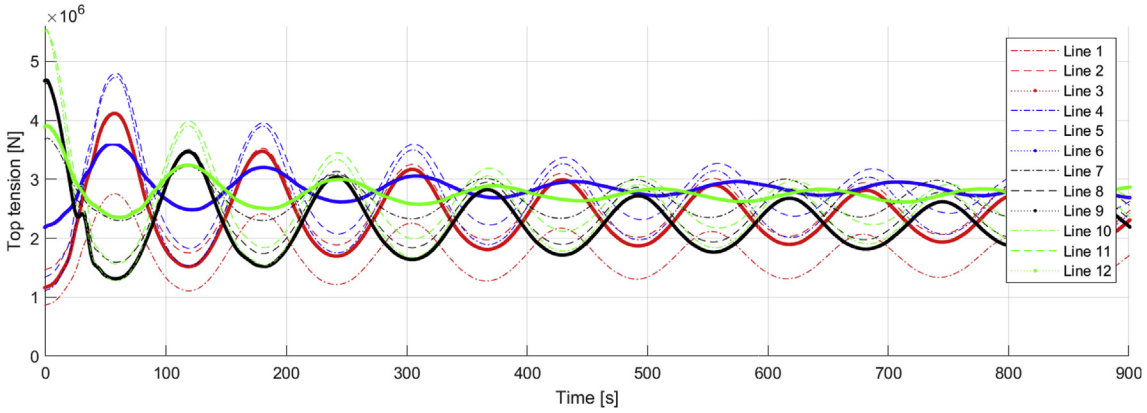

Fig. 12. Output top tensions for 12 mooring lines simulated with RIFLEX during a free decay test.

environmental loadings. This may prove more challenging for the control system, as much higher frequencies of excitation would occur when the system is exposed to environmental forces.

5.3. Nonlinear FE model

The coupling of the nonlinear FE model RIFLEX gave good results, with the static displacement tests giving the expected nonlinear response, and the decay tests showing good repeatability. Given that the general system functionality has been verified above, the primary artefact introduced when using a more complex numerical substructure, is time delays caused by communication from the real-time system to the simulation PC and the numerical calculation time. The time delays induced by using RIFLEX in ReaTHM testing was studied by (Vilsen et al., 2017b). Their impacts on the QoIs implied that time delays induced by the numerical substructure are important performance indicators that must be in focus for future ReaTHM testing applications.

6. Conclusion

The experimental outcomes of this study suggest that the proposed method served as a good guide for how to design a ReaTHM test. Although the method did probably not provide a fully generic setup for ReaTHM testing of ocean structures, it addressed which aspects to consider when designing such tests, and proposed a guideline for how to systematically analyse the considered system.

The outcomes from the case study prove that it is possible to apply nonlinear mooring stiffness from a numerical model onto a physical system in ReaTHM testing of marine structures. However, the method should undergo more extensive validation studies such that the technology can be raised to a TRL-level sufficiently high for the method to be used in design validation of ocean structures.

When testing systems where the vertical force component of the mooring load is of minor importance (e.g. turret-moored Floating Production Storage and Offloading (FPSO) vessels), the ReaTHM testing approach used in this study would be sufficient to apply the correct nonlinear horizontal stiffness and mooring line damping. However, expanding the system to handle more degrees of freedom would enable further applications towards deep water.

Acknowledgements

This work was supported by the Research Council of Norway through the Centres of Excellence funding scheme, Project number 223254 - AMOS, and through the project 254845/O80 “Real-Time Hybrid Model Testing for Extreme Marine Environments” and SINTEF Ocean through the commitment towards the Centre of Excellence - AMOS.

Appendix A

Appendix A.1. Physical model parameters

The Centre of Gravity (COG), the moments of inertia and the gyration radii were found by in-air balancing tests of the model. The metacentric heights (KM) for roll and pitch were found from inclination tests in water. The physical parameters of the cylinder buoy are presented in Table A4.

Table A.4
Parameters of physical substructure determined from model scale testing.

Cylinder parameters		Full-scale	Model-scale
Centre of gravity, vertical position	COG_z [m]	14.8	0.103
Metacentric height, roll	KM-Roll [m]	15.4	0.107
Metacentric height, Pitch	KM-Pitch [m]	15.3	0.106
Moment of Inertia, roll	I_{xx} [kg m^2]	$4.66 \cdot 10^{10}$	0.75
Moment of Inertia, pitch	I_{yy} [kg m^2]	$4.36 \cdot 10^{10}$	0.71
Gyration radius, roll	R_{xx} [m]	23.5	0.163
Gyration radius, pith	r_{yy} [m]	22.8	0.158

Appendix A.2. . Numerical model parameters

The input values for the numerical model are presented (Table A.5).

Table A.5
Numerical model input parameters.

	Length	Area	C_D	C_D	Mass	Number of
	[m]	[m^2]	Longitudinal [-]	Lateral [-]	[kg/m]	elements [-]
Segment 1	52	0.114	0.37	2.4	262.5	7
Segment 2	300	0.141	0.37	1.8	73.90	15
Segment 3	285	0.147	0.37	2.4	436.5	15
Segment 4	930	0.114	0.37	2.4	262.4	23

Appendix A.3. . Kinematic observer

The kinematic observer received input from two sensor systems with different reference frames. The position measurements were made with respect to a local Earth-fixed reference frame, here denoted with subscript *n*, and the accelerations were measured with respect to a body-fixed reference frame denoted with subscript *b*. The observer rotates the acceleration measurements based on the attitude measurements and compensates for gravitational acceleration. The gravity compensated acceleration is then integrated to get the velocity, which is again integrated to get the position. The error between the measured and the estimated position ($\tilde{y}_1$) is used in three feed-back loops on the acceleration bias ($\hat{b}_{acc}$), the rotated acceleration ($\hat{v}^n$) and the estimated linear velocity ($\hat{p}^n$).

$$\dot{\hat{p}}^n = \hat{v}^n + K_1\tilde{y}_1 \tag{A1}$$

$$\dot{\hat{v}}^n = R_b^n(\Theta)[a^b - \hat{b}_{acc}^b] + g^n + K_2\widetilde{y}_1 \tag{A2}$$

$$\dot{\hat{b}}_{acc}^n = K_3 R_b^n(\Theta)^T\tilde{y}_1 \tag{A3}$$

$$\tilde{y}_1 = y_1 - \hat{y}_1 = p^n - \hat{p}^n \tag{A4}$$

$$\hat{v}^b = R_n^b(\Theta)\hat{v}^n \tag{A5}$$

where $\eta = [p^n, \Theta] \in \mathbb{R}^6$ is the position/attitude vectors of the body in the inertial frame of reference. $\nu = [v^b] \in \mathbb{R}^3$ is the body linear velocity vectors, expressed in the body-fixed frame of reference, and $v^n \in \mathbb{R}^3$ is the body linear velocity vector expressed in the inertial frame. $R_b^n(\Theta)$ is the 6 DOF rotation matrix to convert from body-fixed to inertial reference frame. The observer gain matrices K_1, K_2 and K_3 can be tuned such that the error $\tilde{y}_1$ converges exponentially to zero. (Fossen, 2011)

The gravitational acceleration is orders of magnitude larger than the accelerations dynamically induced on the physical substructure. This means that errors in the alignment of attitude and acceleration measurement or time delays between measurements can induce significant errors in the velocity estimation due to the gravity compensation method.

Appendix A.4. Allocation

Pretension was T_0 applied to all lines to prevent these from going slack during testing. The vector force applied from the individual actuation lines is then stated as $f_i = (T_0 + T_i)u_i$ where f_i is the force in line i. $u_i \in \mathbb{R}^3$ is the unit vector spanning from the actuator position to the attachment point on the buoy.

For the horizontal case $\eta = [N, E, \psi] \in \mathbb{R}^3$, the allocation problem can be stated by defining a configuration matrix $A(\eta)$ such that

$$\tau = A(\eta)(T_0 + T) \tag{A.6}$$

This is done by geometric considerations accounting for the actuator positions and the attachment points on the buoy 18. As it is only desired to apply the forces and not the moment, A is reduced to $A_r \in \mathbb{R}^{2x3}$. The configuration matrix expressed as

$$A_r(\eta) = \begin{pmatrix} u_{1,1}(\eta) & \dots & u_{n_l,1}(\eta) \\ u_{1,2}(\eta) & \dots & u_{n_l,2}(\eta) \end{pmatrix} \tag{A.7}$$

The desired line tensions T are then obtained using a pseudo-inverse of the reduced configuration matrix A_r, giving a least squares of T from equation (A.8).

$$T = A_r^{\dagger}(\tau - AT_0) \tag{A.8}$$

$A(\eta)$ does not have full rank at all positions, for instance at $\eta = (0,0,0)$ where the third row of $A(\eta)$ becomes (0,0,0) reducing the rank to 2.

References

Aksnes, V., Berthelsen, P., Fonseca, N., Reinholdtsen, S., 2015. On the need for calibration of numerical models of large floating units against experimental data. In: Proceedings of the 25th International Ocean and Polar Engineering Conference.

Bachynski, E., Chabaud, V., Sauder, T., 2015. Real-time hybrid model testing of floating wind turbines: sensitivity to limited actuation. Energy Procedia 80, 2–12.

E. Bachynski, M. Thys, T. Sauder, V. Chabaud, L. Sæther, Real-time hybrid model testing of a braceless semi-submersible wind turbine. Part 2: experimental results, Proceedings of the ASME 2016 35th International Conference on Ocean, Offshore and Arctic Engineering .

Bayati, I., Belloli, M., Bernini, L., Zasso, A., 2017. Aerodynamic design methodology for wind tunnel tests of wind turbine rotors. J. Wind Eng. Ind. Aerod. 167, 217–227.

Buchner, B., Wichers, J.E.W., de Wilde, J.J., 1999. Features of the state-of-the-art deep-water offshore basin. In: Proceedings of the 31st Offshore Technology Conference. OTC, Houston, Texas, pp. 12 10841.

Cao, Y., Tahchiev, G., 2013. A study on an active hybrid decomposed mooring system for model testing in ocean basin for offshore platforms. In: Proceedings of the ASME 2013 32nd International Conference on Ocean, Offshore and Arctic Engineering, OMAE2013–11471.

Carrion, J.E., Spencer, B.F., 2007. Model-based strategies for real-time hybrid testing, tech. Rep., NSEL, Report No. NSEL-006.
Chabaud, V., 2016. Real-time Hybrid Model Testing of Floating Wind Turbines. PhD Thesis. Norwegian University of Science and Technology.
Chae, Y., Kazemibidokhti, K., Ricles, J.M., 2013. Adaptive time series compensator for delay compensation of servo-hydraulic actuator systems for real-time hybrid simulation. Earthq. Eng. Struct. Dynam. 42 (11), 1697–1715.
de Klerk, D., Rixen, D.J., Voormeeren, S.N., 2008. General framework for dynamic substructuring: history, review, and classification of techniques. AIAA J. 46 (No. 5), 1169–1181.
Faltinsen, O.M., 1990. Sea Loads on Ships and Offshore Structures. Cambridge University Press.
Final Report and Recommendations to the 22nd ITTC, Tech. Rep. The ITTC Specialist Committiee on Deep Water Mooring.
Fossen, T.I., 2011. Handbook of Marine Craft Hydrodynamics and Motion Control. John Wiley & Sons, Ltd.
Horiuchi, T., Nakagawa, M., Sugano, M., Konno, T., 1996. Development of a real-time hybrid experimental system with actuator delay compensation. In: Proc. 11th World Conf. Earthquake Engineering, Paper No. 660.
Horiuchi, T., Inoue, M., Konno, T., Namita, Y., 1999. Real-time hybrid experimental system with actuator delay compensation and its application to a piping system with energy absorber. Earthq. Eng. Struct. Dynam. 28 (10), 1121–1141.
Karnopp, D.C., Margolis, D.L., Rosenberg, R.C., 2006. System Dynamics : Modeling and Simulation of Mechatronic Systems. Wiley.
Nakashima, M., Kato, H., Takaoka, E., 1992. Development of real-time pseudo dynamic testing. Earthq. Eng. Struct. Dynam. 21, 79–92.
Newman, J.N., 1977. Marine Hydrodynamics. The MIT Press 978-0-262-14026-3.
Ocean, S., 2016. RIFLEX 4.8.0 User Manual.
Oguz, E., Clelland, D., Day, A.H., Incecik, A., Lopez, J.A., Sanchez, G., Almeria, G.G., 2018. Experimental and numerical analysis of a TLP floating offshore wind turbine. Ocean Eng. 147, 591–605.
Plummer, A.R., 2006. Model-in-the-loop testing. Proc. Inst. Mech. Eng. I. J. Syst. Contr. Eng. 220 (3), 183–199.
Sauder, T., Chabaud, V., Thys, M., Bachynski, E., Sæther, L., 2016. Real-time hybrid model testing of a braceless semi-submersible wind turbine. Part 1: the hybrid approach. In: Proceedings of the ASME 2016 35th International Conference on Ocean, Offshore and Arctic Engineering, OMAE2017–62498.
Sauder, T., Sørensen, A.J., Larsen, K., 2017. Real-time hybrid model testing of a top tensioned riser: a numerical case study on interface time-delays and truncation ratio. In: Proceedings of the 36th International Conference on Ocean, Offshore and Arctic Engineering. ASME OMAE2017–62498.
Sauder, T., Marelli, S., Larsen, K., Sørensen, A.J., 2018. Active truncation of slender marine structures: influence of the control system on fidelity. Appl. Ocean Res. 74, 154–169.
T. Sauder, S. Marelli, A. J. Sørensen, Probabilistic Robust Design of Control Systems for High-fidelity Cyber-physical Testing, Submitted for Publication.
Stansberg, C.T., Ormberg, H., Oritsland, O., 2002. Challenges in deep water experiments: hybrid approach. J. Offshore Mech. Arctic Eng. 124, 90–96.
Terkovics, N., Neild, S.A., Lowenberg, M., Szalai, R., Krauskopf, B., 2016. Substructurability: the effect of interface location on a real-time dynamic substructuring test. Proc. Math. Phys. Eng. Sci. 472.
Ueland, E.S., Skjetne, R., 2017. Effect of time delays and sampling in force actuated real-time hybrid testing; a case study. In: Proceedings of the OCEANS'17 IEEE/MTS Conference. IEEE/MTS.
Vilsen, S.A., Sauder, T., Sørensen, A.J., 2017a. Real-time hybrid model testing of moored floating structures using nonlinear finite element simulations. chap. 8, ISBN 978-3-319-54930-9, The Society of Experimental Mechanics. Dynamics of Coupled Structures 4, 79–92.
Vilsen, S.A., Føre, M., Sørensen, A.J., 2017b. Numerical models in real-time hybrid model testing of slender marine systems. In: Proceedings of the OCEANS'17 IEEE/MTS Conference. IEEE/MTS.
Vilsen, S.A., Sauder, T., Sørensen, A.J., Føre, M., 2018. Controller analysis in real-time hybrid model testing of an offshore floating system. In: Proceedings of the 37th International Conference on Ocean, Offshore and Arctic Engineering. ASME OMAE2018–77859.